Using Photogrammetry to Evaluate the Failure Mechanisms of Full-Scale Plate Load Testing of Geogrid-Aggregate Composite Layers Placed Over Silty Clay

Benjamin Fox, Kyle Howse, Ian Fleming, Michael Andree & Adam Hammerlindl
Department of Civil, Geological, and Environmental Engineering – University of Saskatchewan, Saskatoon, Saskatchewan, Canada
Bryce Marcotte
SRK Consulting, Saskatoon, Saskatchewan, Canada
Mark Wayne & Andrew Lees
Tensar International, Alpharetta, Gorgia, United States of America

ABSTRACT
Geogrid-aggregate composite layers are used to help improve bearing capacity when working over soft clay. Full-scale plate load testing was done near Clavet, Saskatchewan to better understand the benefits of these stabilised composite layers over soft silty clay. The plate load tests pushed the test pads past their ultimate bearing capacity using a 1m2 steel plate attached to a high-capacity hydraulic cylinder. The hydraulic cylinder was capable of pushing over 1000 kN and was attached below a moveable 60-foot platform which could weigh over 100 tonnes when fully equipped.

Photogrammetry was used as a method to evaluate the failure mechanisms before and after the plate load tests were performed. Photogrammetry involves using computer software to generate a 3-dimensional (3D) surface by taking multiple high-resolution photos from various angles. These 3D surfaces can be used to create digital elevation models (DEMs) which provide a unique opportunity to analyse the failure surfaces of the full-scale plate load tests. Photographs were taken of the top surface before and after every plate load test was pushed. Exhumation of the aggregate material for some of the test pads was done at the end of the season which allowed for additional photographs to be taken of the exposed geogrid layers. The results were used to better understand the failure mechanisms of the geogrid, the volume change caused by heave, and any load spread that might have occurred through the composite layer.

RÉSUMÉ
Les couches composites de géogrille et d'agrégats sont utilisées pour aider à améliorer la capacité portante lors du travail sur de l'argile molle. Des essais de charge de plaque à grande échelle ont été effectués près de Clavet, en Saskatchewan, pour mieux comprendre les avantages de ces couches composites stabilisées sur l'argile limoneuse molle. Les tests de charge de plaque ont poussé les patins de test au-delà de leur capacité portante ultime à l'aide d'une plaque d'acier de 1 m2 fixée à un vérin hydraulique de grande capacité. Le vérin hydraulique était capable de pousser plus de 1000 kN et était fixé sous une plate-forme mobile de 60 pieds qui pouvait peser plus de 100 tonnes lorsqu'elle était entièrement équipée.

La photogrammétrie a été utilisée comme méthode pour évaluer les mécanismes de défaillance avant et après la réalisation des tests de charge de plaque. La photogrammétrie consiste à utiliser un logiciel informatique pour générer une surface tridimensionnelle (3D) en prenant plusieurs photos haute résolution sous différents angles. Ces surfaces 3D peuvent être utilisées pour créer des modèles numériques d'élévation (DEM) qui offrent une occasion unique d'analyser les surfaces de rupture des essais de charge de plaque à grande échelle. Des photographies ont été prises de la surface supérieure avant et après chaque essai de charge de plaque. L'exhumation du granulat pour certaines des plates-formes d'essai a été effectuée à la fin de la saison, ce qui a permis de prendre des photographies supplémentaires des couches de géogrille exposées. Les résultats ont été utilisés pour mieux comprendre les mécanismes de défaillance de la géogrille, le changement de volume causé par le soulèvement et toute répartition de charge qui aurait pu se produire à travers la couche composite.

1 INTRODUCTION

Geogrids stabilisation is becoming more common in industry, including applications such as road construction, temporary crane pads, and railway ballasts. Geogrid stabilisation is relatively novel and many new geogrid products are specialising in this field, including triangular (Lees and Clausen, 2020) and variable aperture size geogrids. The primary mechanism of stabilisation is the interlocking effect that the geogrid has with the surrounding aggregate material (Bussert and Cavanaugh 2010, Byun et al 2019, Lees and Clausen 2020, Liu et al 2017). Aggregate that is interlocked within the apertures of the geogrid also interlocks adjacent particles, which creates a stabilisation gradient. This gradient has been shown to

extend up to 300 mm past the geogrid layer (Bussert and Cavanaugh 2010).

There have been many laboratory testing experiments on geogrid-aggregate composite layers (Love et al. 1987, Roy and Deb 2017, Sun et al. 2018) and few full scale experiments (Demir et al. 2013). Of those experiments, measurements of heave, load spreading, and geogrid rupture mechanisms of the composite layer have been ignored or difficult to obtain.

In this study, large scale plate load testing of geogrid stabilised aggregate layers was conducted near Clavet, Saskatchewan during 2019, 2020, and 2021. The tests involved pushing a 1m^2 plate into geogrid stabilised pads until ultimate bearing capacity was reached. The pads were constructed in 5 m wide trenches, and the hydraulic cylinder used for testing was attached below a large moveable steel platform (Figure 1). Two different geogrid-aggregate composites were used, thinner layers (0.25 m and 0.3 m) with one geogrid at the subgrade-aggregate interface, and thicker layers (0.5 m and 0.6 m) with a geogrid at the interface as well as in the middle of the aggregate layer.

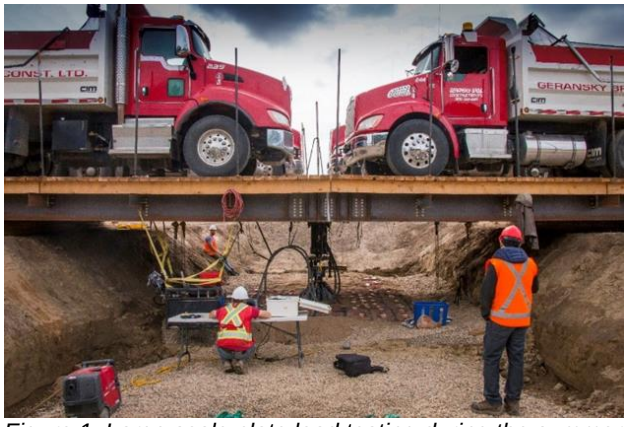

Figure 1: Large scale plate load testing during the summer of 2019.

Photogrammetry was used to make 3D models of the surface and subsurface layers to better understand the characteristics of the plate load tests. The 3D models were generated with Agisoft Metashape by using upwards of 150 high-resolution digital images of the surfaces before and after plate load testing. The 3D models were georeferenced, allowing them to be compared against each other. Digital elevation models (DEM) were created from the 3D models and analysed using Python. Analysis of the plate load test using photogrammetry includes grid rupture, load spread angles, and volume change from heave.

2 FIELD WORK

Photogrammetry of the top-most surface was done before and after all 51 plate load tests were pushed. Photogrammetry of the exhumed layers was done at the end of the field season. As the excavation process was labour intensive, 28 of the 51 plate load tests were exhumed to the location of the geogrid stabilizing layers.

Several flat cardboard targets with survey prisms attached at the centre (Figure 2) were placed approximately 4 m away from the centre of the plate load tests. Placing the targets away from the plate load test was done to reduce disturbance from heave during plate load testing. The coordinates of the prisms on the targets were used to georeference the processed surfaces in 3D space. Coordinates of the prisms were taken using a georeferenced automatic total station (Leica TS16) located above the trench wall. The cardboard surface of the targets has alignment points and unique patterns to facilitate post processing.

Figure 2: Targets equipped with prisms used to georeference photogrammetry models.

Photos of the surface were taken sequentially and at different angles, with more photos taken at the target locations. A Canon EOS 70D with a EFS 18 – 135 mm lends was used, and settings were adjusted at the beginning of each session to maximize the clarity of the photos. The zoom of the camera lens was fixed to minimise distortion effects between the images. A visual representation of the camera locations can be seen on Figure 3, where the blue boxes each represent a camera location and orientation.

The ground surface was spray painted with different patterns, including test names, to introduce unique visual features to help the software align the photos. Maintaining consistent lighting conditions for the photos was challenging and involved diffusing bright sunlight with tarps when necessary. Stepping on the heave surface between photogrammetry trials and during plate load testing was avoided to reduce disturbance.

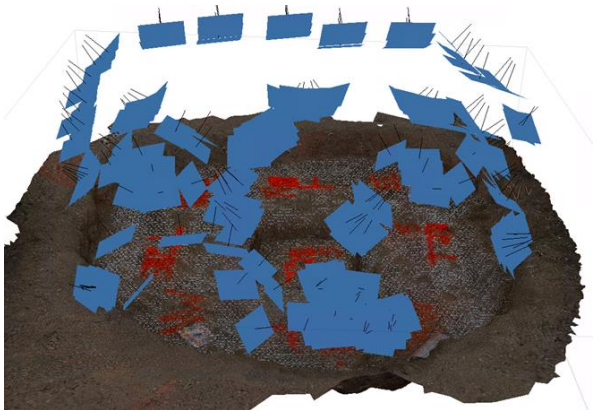

Figure 3: Camera angles and locations for a typical surface analysis.

Exhumation of the aggregate surfaces for a select number of plate load tests was done after all of the plate load tests were pushed and before site reclamation took place. In 2019, excavation was done manually by shovelling material from the test area. Exhumation in 2021 was done using a vacuum truck (Figure 4) to remove the material from the trench by first using a hammer drill to break up the packed material. In both cases, once the interface layer had been exposed, care was taken to not disturb the surface heave or geogrid layer.

Although disturbing the surface was avoided, it is likely that there was a reduction of heave because of the exhumation process. When exhuming, it was not possible to avoid standing on the heave surface, which would inevitably change the original surface conditions.

Figure 4: Vacuum truck used to exhume interface surfaces in 2021.

3 POST PROCESSING

Agisoft Metashape professional was used to create the 3D surface models. The required steps to create the model are to align the photos, build a mesh, build a dense point cloud, and to generate texture for the model.

After the model was generated, the cardboard targets were used to georeferenced the model. As seen in Figure 5, because the prism is thin and tall, the prism generated by the model usually did not have enough detail to be used for georeferencing. Each target had four markers on the cardboard surface, which were located on each side of the prism. The centre of the prism was found by taking the intersection point of the lines that connect the markers (Figure 5) and adjusting the height by the height of the prism. After the model was generated and georeferenced, a scale bar with a known length was used to check the accuracy of the model.

Figure 5: The inaccuracies of the prism (left) and the method to obtain the proper coordinate of the prism (Right).

Although pre- and post-surface photos were taken for each plate load test, many of the photogrammetry models could not be used. The most common source of error came from inaccurate representation of the targets. This could be caused by inconsistent lighting, an insufficient number of photos, or not enough variation in the angles of the photographs. Without being able to use the targets as georeferenced points, there was no way to reliably scale and orientate the model.

Generating and georeferencing these models allowed for a wide range of analysis to be conducted, which included heave extent and volume change, geogrid rupture observations, and load spread angle approximation.

4 HEAVE AND VOLUME CHANGE

Using photogrammetry to analyse heave can be a practical alternative to traditional methods, which usually involve multiple displacement transducers over a large area (e.g., Palmeira and Antunes 2010). Not only is photogrammetry capable of providing data for the entire surface without the need to interpolate between points, but it is also nonobtrusive, which reduces disturbances such as installing instrumentation.

Slaker et al. (2018) used photogrammetry to analyse heave in a limestone mine in eastern Ontario. The heave obtained from the photogrammetry in their experiment was compared with known displacements from extensometers at specific locations. Although some of the results were promising, many of the extensometers did not match photogrammetry displacements. There were several factors that could have caused inconsistency, including lighting conditions and lack of variability in the photos, but one of the main sources of error was that each photogrammetry file was compared against the initial survey. Without points to georeference each set of photos, it is difficult to accurately represent the model in 3D space,

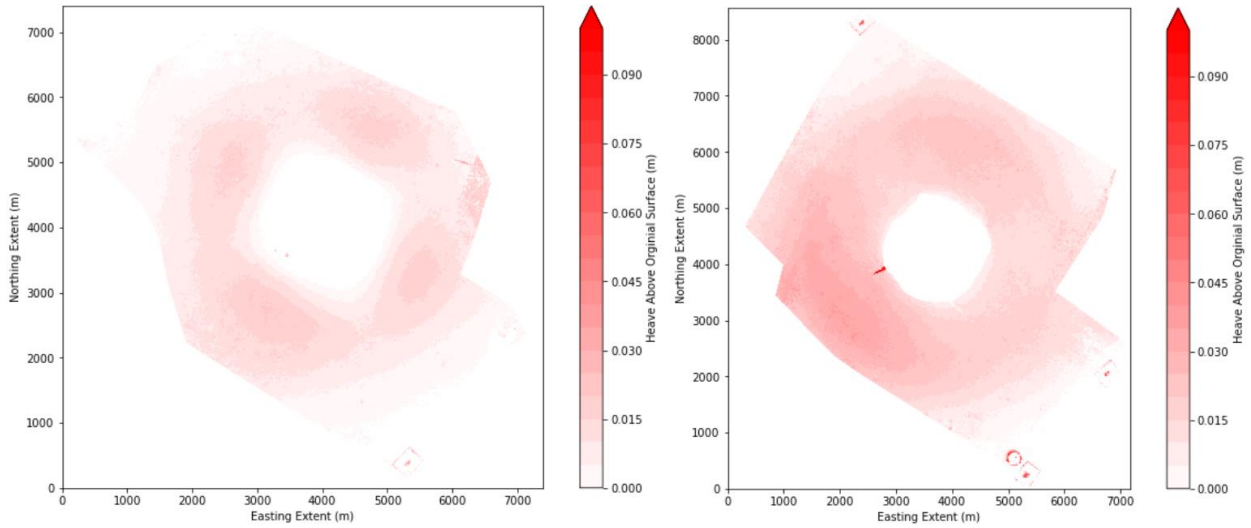

Figure 6: Unstabilised (left) and stabilised (right) changes in surface elevation from a plate load test.

especially if there are long periods of time between photogrammetry sessions.

Georeferenced surface elevation data for before and after a plate load test was pushed was needed to be able to analyse the heave generated during a plate load test. Digital elevation models (DEM) were created and exported from Agisoft Metashape as TIFF files containing unique points with unique values for latitude, longitude, and elevation. The inner and outer boundaries of the DEMs were manually outlined using polygons to be able to exclude parts of the model that were not properly rendered.

A Python script interpolated the DEMs onto a regular grid, and then calculated the difference between the DEMs generated from before and after a plate load test was pushed. The resulting DEM showed the severity and extent of heave that surrounded the plate. Since the targets were in the same location before and after the plate load tests, the targets were used as a reference point to make sure the python code properly subtracted the elevations. If the targets all showed excessive negative or positive elevation change after subtraction, the script was able to move the DEMs closer to one another by a set value.

An example of the difference between a 0.6 m stabilised and unstabilised pad can be seen in Figure 6. The results demonstrate that the geogrid-stabilised layers distribute the heave further across the surface than the unstabilised pads. This could be a result of the load surcharge transfer mechanism described by Lees (2017). The increased heave is likely caused by the higher loads applied to the stabilised bearing pads compared to the unstabilised bearing pads.

One way to be able to quantify the heave that occurred from the plate load tests is to calculate the produced volume change. Each data pixel of a DEM has three components, lattitude, longitude, and elevation. Each one of these pixels has a resolution, which defines how much space the point occupies. Higher resolution results in higher accuracy of the calculated volume change. The volume change was calculated in a Python script by summing the volume of all pixels of a DEM. This was done for the DEMs produced by subtracting the pre-heave and post-heave surfaces. Both negative and positive volume change could be calculated.

Calculating the volume change can provide useful information about the characteristics of the plate load tests. If the system was fully undrained, then the volume displacement from the plate load test should be approximately equal to the heave that occurred at the surface. If there was no volume change at the surface, then the subgrade might have been unsaturated. Volume change calculations can also act as a means of quantifying the surcharge load transfer that results from having stabilised testing pads.

5. GEOGRID RUPTURES

Geogrid rupture mechanisms were observed for two different types of grid-aggregate composites. The first type of composite layer was a triangular aperture geogrid with a coarse uniform 19mm crushed rock. The second was a variable aperture geogrid with a custom graded aggregate, which is similar to a type of road base used in the United Kingdom. Examples of the photogrammetry models for both types of geogrid can be seen in Figure 7. The geogrid used for the 19mm composite layer was black, making it more difficult to distinguish from shadows and the surrounding material.

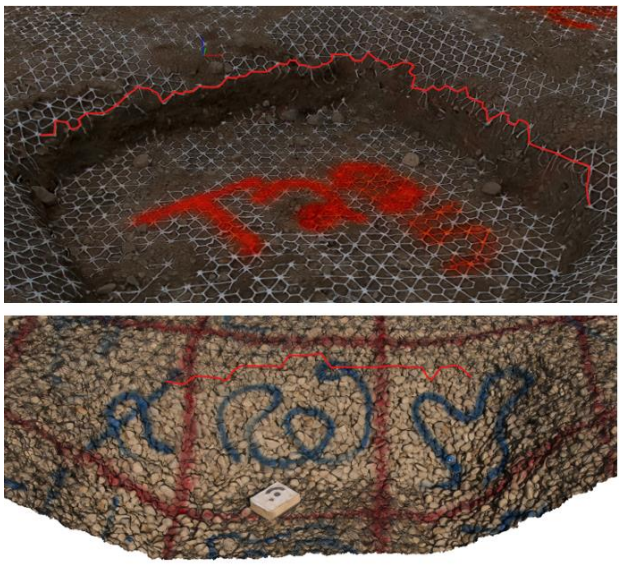

Figure 7: Grid rupture analysis

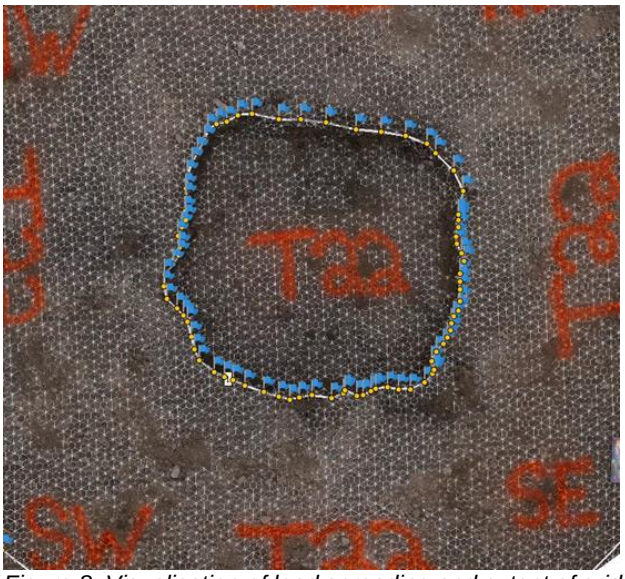

Figure 8: Visualisation of load spreading and extent of grid rupture from an exhumed layer.

The failure planes and geogrid strains can be better understood by analysing the exhumed models. Observations of the failure planes demonstrate that the variable aperture geogrid had no noticeable failure plane, but the triangular aperture geogrid was more likely to fail in a straight line along a set of nodes. There were also cases for the triangular aperture geogrid where the grid on one edge of the exhumed plate imprint did not rupture, which further suggests that there were planes of failure. The variable aperture geogrid has several different size ribs in various directions, which could prevent rib failure from propagating.

6. LOAD SPREAD

A traditional method for calculating bearing capacity is the load spread method proposed by Terzaghi and Peck (1948). The method uses the load spread angle, which is the angle from the edge of the bearing surface to the extent that the load acts on the subgrade. Load spread angles were calculate by using the rupture area of the geogrid after exhumation. The area was found by calculating the area of a manually placed polygon that follows the rupture pattern of the geogrid (Figure 8). Once the area was known, an equivalent side length was calculated by assuming the area as a square. Using the equivalent side length, the angle from the 1m^2 plate to the edge of the new equivalent square can be calculated.

This method provides a general idea for how the load might be spread through the aggregate during a plate load test, but there is uncertainty with the applicability of results. Load spreading is likely to change as the displacement of the plate pushing into the ground, and the distance from the plate to the grid at rupture can be difficult to predict.

Some research has showed that load spreading is difficult to express as an angle because the distribution of load on the subgrade surface dissipates as you get further from the initial contact area (Madhav and Sharma 1991). A summary by Chua and Nepal (2022) demonstrates how the load spread angle can vary from 8.4 (Young and Focht 1981) to 26.6 (Terzaghi and Peck 1948) and can be as high as 45 for geogrid stabilised pads (Palmeira and Antunes 2010).

It should also be mentioned that there was no photogrammetry with cases without grid for the variable aperture geogrid trials. Exhumation of the controls for the 19mm aggregate was manageable because of the noticeable difference between the two materials, but the interface between the road base material and the subgrade was a lot more difficult to obtain.

7. CONCLUSION

Photogrammetry was used to analyse large scale plate load testing done at Clavet, Saskatchewan during 2019, 2020, and 2021. The plate load testing involved pushing a 1m^2 steel reinforced plate into geogrid-stabilised aggregate pads overlying soft silty clay. The tests were pushed past their ultimate bearing capacity by a hydraulic cylinder capable over pushing over 100 tonnes. Triangular and variable aperture geogrids were used during testing, with two different types of aggregates.

Upwards of 150 high-quality surface photos were taken before and after plate load testing for all 51 tests. 28 of the tests were also exhumed to obtain surface profiles of

the geogrid layers, and 9 of which had a layer within the aggregate as well as at the aggregate-subgrade interface. The surface models and DEMs generated from photogrammetry were georeferenced so that proper scaling and orientation could be achieved. Heave, load spreading angles, and grid rupture analysis were possible with the photogrammetry results.

Surface heave analysis was done by subtracting the DEMs created from before and after a plate load test was pushed. Volume change from heave was calculated for each generated DEM and compared to the volume change obtained from the total displacement of the plate load test. Although the results are preliminary, the produced heave was distributed over a larger area for the geogrid stabilised pads compared to the unstabilised pads. Further analysis of the heave results can be done to evaluate the drained or undrained behaviour of the subgrade material.

Geogrid rupture patterns were used to observe load spreading angles. The load spread angle is difficult to quantify, particularly because the load spread angle can change based on proximity of the plate to the geogrid layer during testing. In this analysis, load spread angles were calculated at failure, when the plate might have been much closer to the geogrid layer.

The exhumed layers were also used to observe grid rupture mechanisms. Preliminary results for grid rupture show that the variable aperture geogrids had a less noticeable failure plane, whereas the triangular aperture geogrid exhibited propagated failure.

8. ACKNOWLEDGEMENTS

The authors would like to acknowledge Tensar International for providing funding for this project, as well as ConeTec, Machibroda Engineering Ltd., and the Livestock Forage and Research Centre of Excellence for their equipment, volunteer work, and workspace. Further acknowledgments are extended to the staff and students of the geotechnical lab at the University of Saskatchewan.

9. REFERENCES

AgiSoft Metashape Professional. Version 1.7.2. 2020. Retrieved from http://www.agisoft.com/downloads/installer/

Bussert, F., & Cavanaugh, J. 2010. *Recent research and future implications of the actual behavior of geogrids in reinforced soil.* In Earth Retention Conference 3 (pp. 460-477).

Byun, Y.H., Tutumluer, E., Feng, B., Kim, J.H. and Wayne, M.H., 2019. *Horizontal stiffness evaluation of geogrid-stabilized aggregate using shear wave transducers.* Geotextiles and Geomembranes, 47(2): 177-186.

Chua, B. T., & Nepal, K. P. 2022. *A New Approach to Estimate Bearing Capacity of Strip Footings on Geogrid-Stabilised Granular Layer over Clay.* Transportation Infrastructure Geotechnology, 1-26.

Demir, A., Laman, M., Yildiz, A., & Ornek, M. 2013. *Large scale field tests on geogrid-reinforced granular fill underlain by clay soil.* Geotextiles and Geomembranes, 38, 1-15.

Lees, A. 2017. *Simulation of geogrid stabilisation by finite element analysis.* In Proceedings of the 19th International Conference on Soil Mechanics and Geotechnical Engineering, Seoul, 1377-1380.

Lees, A. S., & Clausen, J. 2020. Strength envelope of granular soil stabilized by multi-axial geogrid in large triaxial tests. Canadian Geotechnical Journal, 57(3), 448-452.

Liu, S., Huang, H., & Qiu, T. 2017. *Behavior of geogrid-reinforced railroad ballast particles under different loading configurations during initial compaction phase.* ASME/IEEE Joint Rail Conference, American Society of Mechanical Engineers, Philadelphia, Pennsylvania, 50718: V001T01A002

Love, J. P., Burd, H. J., Milligan, G. W. E., & Houlsby, G. T. 1987. *Analytical and model studies of reinforcement of a layer of granular fill on a soft clay subgrade.* Canadian Geotechnical Journal, 24(4), 611-622.

Madhav, M. R., & Sharma, J. S. N. 1991. *Bearing capacity of clay overlain by stiff soil.* Journal of geotechnical engineering, 117(12), 1941-1948.

Palmeira, E. M., & Antunes, L. G. 2010. *Large scale tests on geosynthetic reinforced unpaved roads subjected to surface maintenance.* Geotextiles and Geomembranes, 28(6), 547-558.

Slaker, B. A., Murphy, M. M., & Miller, T. 2018. *Analysis of extensometer, photogrammetry and laser scanning monitoring techniques for measuring floor heave in an underground limestone mine.* Transactions of Society for Mining, Metallurgy, and Exploration, Inc, 344(1), 31.

Sun, X., Han, J., Parsons, R.L., and Thakur, J. 2018. *Equivalent California Bearing Ratios of Multiaxial Geogrid-Stabilized Aggregates over Weak Subgrade.* Journal of Materials in Civil Engineering, 30(11): 04018284.

Terzaghi, K., & Peck, R. B. 1948. *Soil Mechanics. Engineering Practice.* John Wiley and Sons, Inc., New York.

Young, A. G., & Focht, J. A. 1981. *Subsurface hazards affect mobile jack-up rig operations.* Soundings, 3(2), 4-9.